Abnormal Grain Growth in Bulk Cu—The Dependence on Initial Grain Size and Annealing Temperature

JAE BON KOO and DUK YONG YOON

The dependence of abnormal grain growth (AGG), also termed secondary recrystallization, on annealing temperature in the range between 600 °C and 1050 °C has been observed in pure bulk Cu specimens compressed to various levels between 5 and 75 pct. There is no grain texture after annealing. The average grain size after primary recrystallization, which represents the initial grain size for secondary recrystallization during further annealing, decreases with increasing deformation and is nearly independent of the annealing temperature, in agreement with previous observations. The incubation time for AGG decreases and the number density of abnormally large grains increases with increasing deformation (hence, a decreasing initial grain size) and increasing annealing temperature. At low temperatures, most of the grain boundaries are faceted, with some facet planes probably of singular structures corresponding to cusps in the polar plots of the grain-boundary energy *vs* the grain-boundary normal. With increasing temperature, the grain boundaries become defaceted and, hence, atomically rough. The observed grain-growth behavior appears to be qualitatively consistent with the movement of faceted grain boundaries by two-dimensional nucleation of boundary steps. The temperature dependence appears to be consistent with roughening of grain boundaries. Before the onset of AGG, stagnant growth of the grains occurs at low rates, probably limited by slow two-dimensional nucleation of boundary steps, and, at low deformations and low annealing temperatures, the stagnant growth persists for 100 hours. The specimens with relatively small initial grain sizes (because of high deformation) show double AGG when annealed at high temperatures.

I. INTRODUCTION

IF a deformed polycrystal is annealed further after completion of the primary recrystallization, the grains coarsen because of the grain-boundary energy. Such a grain growth often occurs abnormally and is usually called secondary recrystallization.[1] In this report, we will use both terms, abnormal grain growth (AGG) and secondary recrystallization, interchangeably, because AGG after the primary recrystallization is our main subject. The secondary recrystallization has been observed in many pure metals such as Fe,[2] Cd,[3] Pb,[3] Zn,[4] Cu,[5,6] Ni,[7,8] and Ag,[9,10,11] as well as in alloys. In Ni,[8] Ag,[11] and single-phase alloys[12,13] without any notable textures, AGG was observed to occur at relatively low temperatures when most of the grain boundaries were found to be faceted. At high temperatures close to the melting points in certain atmospheres, the grain growth was found to be normal, with all of the grain boundaries defaceted and, hence, atomically rough.[8,11–14] Such a correlation between the grain-boundary structure and the grain-growth behavior was also found in such oxides as $BaTiO_3$[15] and Al_2O_3.[16]

Because at least some segments of the faceted grain boundaries were likely to be singular with atomically flat structures, it was proposed[8,11,17] that AGG occurred because the faceted grain boundaries moved by either two-dimensional nucleation of boundary steps or by growth on the steps produced by dislocations, in analogy to the AGG of polyhedral grains in liquid[18] or vapor.[19,20] Because at high temperatures the defaceted grain boundaries have atomically rough structures, they move continuously, resulting in normal growth behavior. In Ni[8] and Ag,[11] the incubation time for AGG was observed to decrease and the number density of abnormal grains was observed to increase as the annealing temperature increased, and Yoon *et al.*[17] suggested that such a temperature dependence was consistent with the step-growth mechanism if the grain-boundary-roughening transition was taken into account.

The purpose of this work is to observe the dependence of AGG in bulk Cu on initial grain size and annealing temperature. Bulk Cu was selected because of its own importance, as well as for a model of other polycrystalline materials. Because the AGG behavior depends critically on both of these variables, it was necessary to study their effects simultaneously. The initial grain size for AGG is the grain size obtained after primary recrystallization, which was found to vary with deformation but to be nearly independent of the annealing temperature in α-brass[21] and other metals.[22,23] Experimentally, therefore, we will observe the dependence of the secondary recrystallization behavior on deformation and annealing temperature.

The abnormal grain growth has been observed in both bulk and thin films of Cu. Kronberg and Wilson[5] found that when a heavily cold-rolled thin Cu plate was annealed at temperatures between 400 °C and 1050 °C, cubically aligned grain textures appeared and the abnormally growing large grains had a coincidence-site lattice-orientation relationship to the grains formed during primary recrystallization. The size of the abnormally growing grains was observed to decrease with increasing heating rate to the annealing temperatures, and the incubation time for the initiation of

JAE BON KOO, formerly Graduate Student, Department of Materials Science and Engineering, Korea Advanced Institute of Science and Technology, is Associate Researcher, Samsung SDI Co., Ltd., Suwon 442-731, Korea. DUK YONG YOON, Professor, is with the Department of Materials Science and Engineering, Korea Advanced Institute of Science and Technology, Taejon 305-701, Korea.

Manuscript submitted May 25, 2000.

AGG was observed to decrease with increasing annealing temperature. But the evolution of the grain structure during the annealing treatments was not presented, and, thus, the dependence of AGG on annealing temperature could not be fully characterized.

Çigdem[6] investigated AGG in bulk Cu deformed to various strains up to 15 pct, but the annealing was done in a narrow temperature range of 550 °C to 650 °C and only for 1 hour. He observed a large change of the average grain size with deformation, but the results were inadequate to fully characterize the dependence of AGG behavior on deformation and annealing temperature. In thin films formed by deposition, there has apparently been no attempt to systematically vary the initial grain size. Unlike the bulk specimens, textures usually develop in thin films, and the AGG behavior is believed to be determined by the surface energy and stress.[24,25,26]

Also in other polycrystalline materials, a systematic study of the dependence of secondary recrystallization on deformation and annealing temperature is still lacking. In Fe[2,27,28] and stainless steel,[29] for example, the observations were limited to the effects of low deformations, which were below the levels required for recrystallization. In a Si-steel plate with a characteristic Goss texture, Woo *et al.*[30] reported that the annealing temperatures required for AGG increased with the grain size obtained after the primary recrystallization. Their micrographs also showed that after 1 hour of annealing treatments, the average size of the abnormally growing grains, apparently after their impingement with each other, decreased with increasing deformation and annealing temperature.

It is necessary to produce and examine many specimens to fully characterize the dependence of secondary recrystallization on deformation, annealing temperature, and annealing time. These three experimental variables were, therefore, judiciously selected in this work to reveal the critical changes in the grain-growth behavior. The deformation was carried out in such a way as to eliminate any texture in the bulk specimens. The deformations were mostly above the level required for primary recrystallization. We will attempt to show that the step-growth mechanism provides a qualitative framework for explaining the relatively complex dependence of the secondary recrystallization on deformation, annealing temperature, and annealing time.

II. EXPERIMENTAL PROCEDURE

Copper cylinders of 99.9999 pct purity, 11 mm in diameter and 20 mm in length, were compressed to a 30 pct reduction in length and annealed at 500 °C for 30 minutes in vacuum to obtain a recrystallized microstructure of fine grains. The Cu cylinders were then compressed to 5, 10, 20, 35, 50, 65, and 75 pct reductions in length. The specimens were rapidly pushed into the center of a tube furnace preheated to 600 °C, 700 °C, 800 °C, 900 °C, 950 °C, or 1050 °C, annealed for various periods in a vacuum of 10^{-4} to 10^{-5} torr, and quenched in water. The annealed specimens were sectioned perpendicular to their axes and through their centers for microscopic observations. The polished surfaces were etched in a solution of 50 mL hydrochloric acid, 75 mL ethyl alcohol, 75 mL water, and 10 g copper (II) sulfate pentahydrate. The grain-boundary morphology was examined by optical microscopy, scanning electron microscopy (SEM), and transmission electron microscopy (TEM). The equivalent sphere diameters of the grains were measured by tracing along the grain boundaries on micrographs using a digitizer connected to a personal computer. About 300 grains were randomly selected in each specimen to determine the average grain size and grain-size distribution.

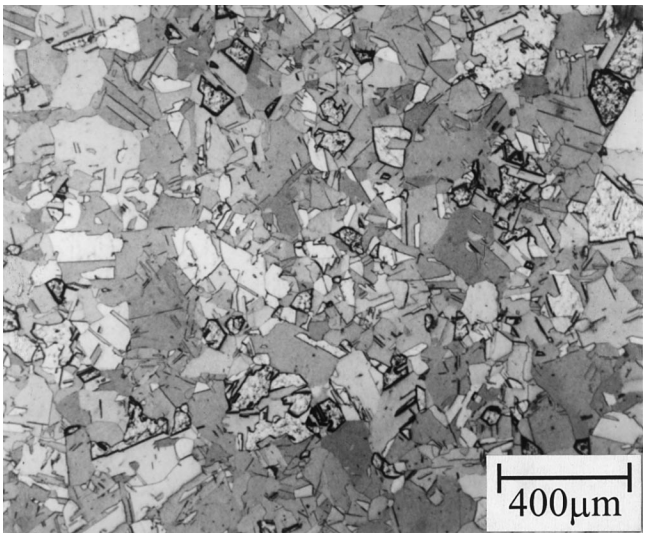

Fig. 1—The optical microstructure of the specimen annealed at 500 °C for 30 min after 30 pct compression representing the initial structure for all subsequent deformation and annealing experiments.

III. RESULTS AND DISCUSSION

The as-received Cu cylindrical rods had grains of about 500 μm in diameter and with somewhat irregular shapes, but without any twins. After compressing to a 30 pct reduction in height and annealing at 500 °C for 30 minutes, grains of about 200 μm in average size were obtained, as shown in Figure 1. When the specimens with the structure shown in Figure 1 were again compressed to various levels and annealed at various temperatures, most of them showed primary recrystallization and, subsequently, AGG. The specimen series deformed to a certain level and annealed at a given temperature for various times will be designated by its deformation/temperature. Thus, the specimen series deformed to 50 pct and annealed at 800 °C is designated as 50 pct/800 °C. Each specimen will be designated by deformation/temperature/time; thus, 50 pct/800 °C/1 min designates the specimen deformed to 50 pct and annealed at 800 °C for 1 minute.

The local strains at various points of the compressed specimens were estimated by finite-element analysis. The strains at the center of the specimens, where the microstructural observations were made, were found to be fairly uniform and slightly higher than the compression in height. The microstructures observed after the annealing treatments were, indeed, found to be fairly uniform in this zone.

A typical recrystallization and AGG behavior was observed in the 50 pct/800 °C series, as shown in Figure 2. After annealing for 1 minute (Figure 2(a)), primary recrystallization appeared to be complete, with an average grain size of about 38 μm, which is much smaller than that shown in Figure 1. (The grain size is the approximate diameter, or

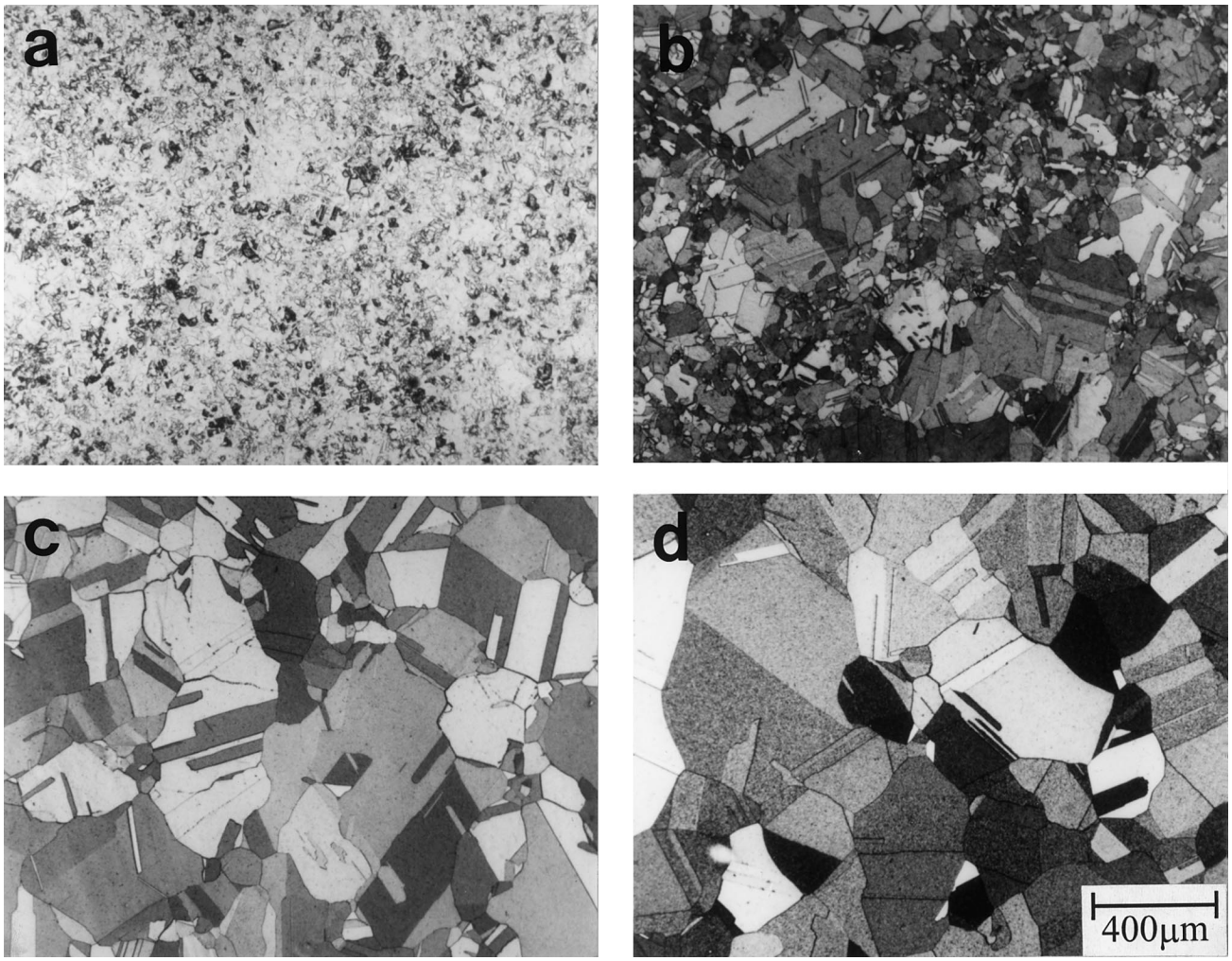

Fig. 2—The optical microstructures of the specimens annealed at 800 °C for (*a*) 1 min, (*b*) 4 min, (*c*) 10 min, and (*d*) 24 h after 50 pct compression.

the equivalent sphere diameter when given numerically.) The termination of the primary recrystallization (and, hence, the beginning of the secondary recrystallization) was determined by the appearance of grains with distinct grain boundaries. In some specimen series, it was also confirmed by measuring the Vickers microhardness with a diamond pyramid head of about 1 mm size. The Vickers hardness number of the specimen after deforming to 50 pct was 145, and after annealing at 800 °C for 1 minute, it decreased to 68. During further annealing, it gradually decreased and became 55 after 24 hours. These values are close to the Vickers hardness number of 58 to 62 reported earlier[6] for fully annealed Cu. Therefore, for the 50 pct/800 °C series, it was decided that the primary recrystallization was complete after 1 minute, with the grain structure shown in Figure 2(a). For this specimen, the presence of distinct grain boundaries and the absence of many dislocations produced by deformation were confirmed by observations using TEM.

As expected from the previous observations in single-phase materials,[21,22,23] the grain size after the primary recrystallization at 800 °C was found to sharply decrease with increasing deformation, as shown in Figure 3. In the specimen series compressed to 10 pct, for example, the recrystallization did not appear to be complete after annealing for 7 minutes at 800 °C, but after 15 minutes it appeared

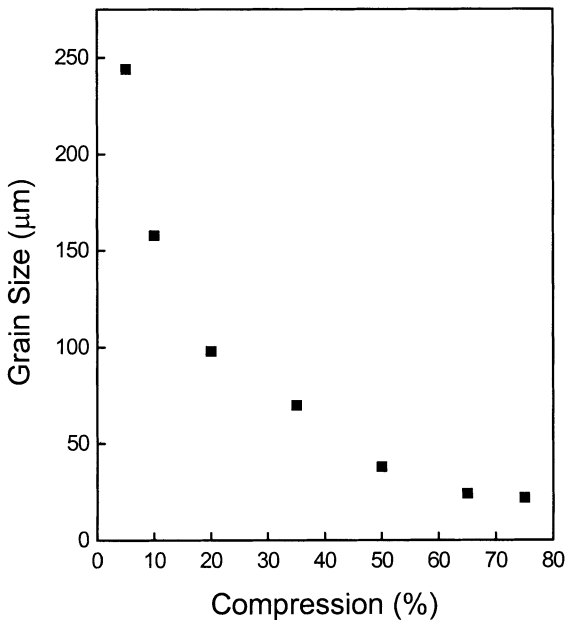

Fig. 3—The variation of the average grain size after primary recrystallization at 800 °C with the level of compression.

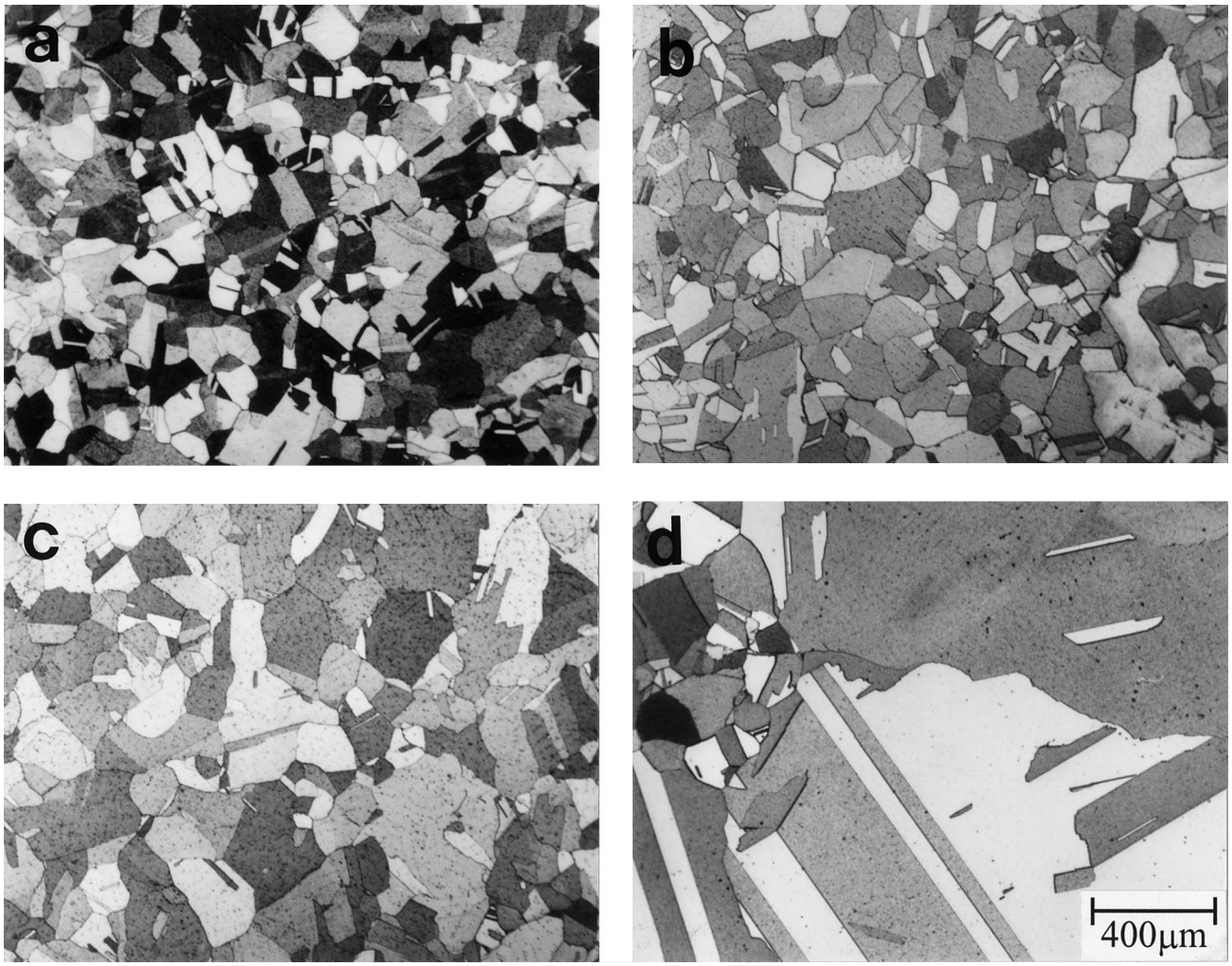

Fig. 4—The optical microstructures of the specimens annealed at 800 °C for (*a*) 15 min, (*b*) 30 min, (*c*) 2 h, and (*d*) 24 h after 10 pct compression.

to be complete, with a Vickers hardness of 66. As shown in Figure 4(a), the grain size was 158 μm, which was smaller than the initial size (about 200 μm) shown in Figure 1. In the specimen compressed to 5 pct, it was not clear if recrystallization occurred, but after annealing for 1 hour at 800 °C (Figure 10(b)), distinct grain boundaries appeared, with a Vickers hardness of 61. Therefore, this was selected to represent the initial state for the subsequent grain growth. Because the primary recrystallization was not the main objective of this work, completion of the primary recrystallization was not precisely determined using fine time intervals for the annealing treatments. Therefore, the average grain sizes shown in Figure 3 represent only approximately the initial values for subsequent grain growth. The actual values could be slightly smaller than these, because these were obtained from the specimens where the termination of primary recrystallization appeared to be quite certain.

All of the specimens compressed to various levels between 10 and 75 pct showed AGG during annealing at 800 °C, as shown by the examples of Figures 2 and 4 for those compressed to 50 and 10 pct, respectively. In the specimens compressed to 50 pct, AGG occurred after annealing for 4 minutes (Figure 2(b)), with some grains growing to sizes as large as about 400 μm, while the matrix grains were still fine. After 10 minutes (Figure 2(c)), AGG appeared to be nearly complete, with the large grains impinging upon each other. When annealed further for 24 hours (Figure 2(d)), the smaller grains disappeared and the large grains grew slightly, to an average size of about 650 μm. The X-ray pole figures of these specimens were compared to that of a Cu powder compact in order to determine the grain textures. The specimen compressed to 50 pct had a slight deformation texture, but none of the annealed specimens showed any texture. This result agrees with the previous observations[31,32] that even rolling below 80 pct does not produce any texture after annealing treatments.

The grain-boundary shapes in various specimens were examined under either TEM, when the grains were relatively fine, or under SEM, when the grains became relatively large by AGG. The grain boundaries in the specimens annealed at 800 °C showed pronounced faceting. The grain boundaries faceted at relatively large scales are indicated by the numbers 1 through 6 in Figure 5(a) for the 5 pct/800 °C/24 h specimen, and their faceted structures were verified at a higher magnification under SEM, as shown for two of these in Figures 5(b) and (c). It is likely that the other grain boundaries, which appeared to be smoothly curved in Figure 5(a), were also faceted at finer scales. The TEM observations showed that about 60 to 70 pct of the grain boundaries in the 50 pct/800 °C/1 min specimen (Figure 2(a)) were faceted, as

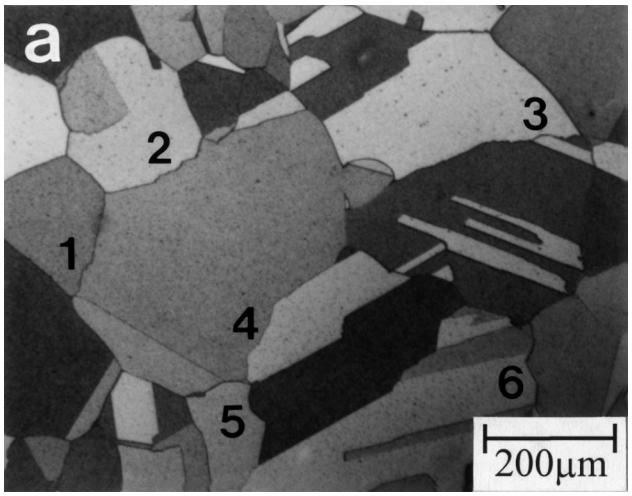

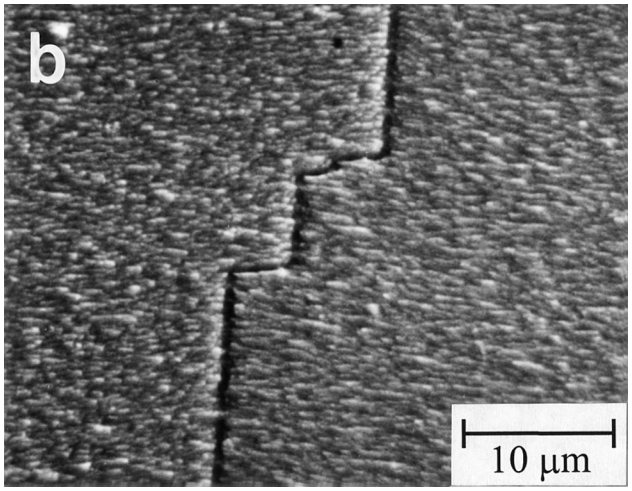

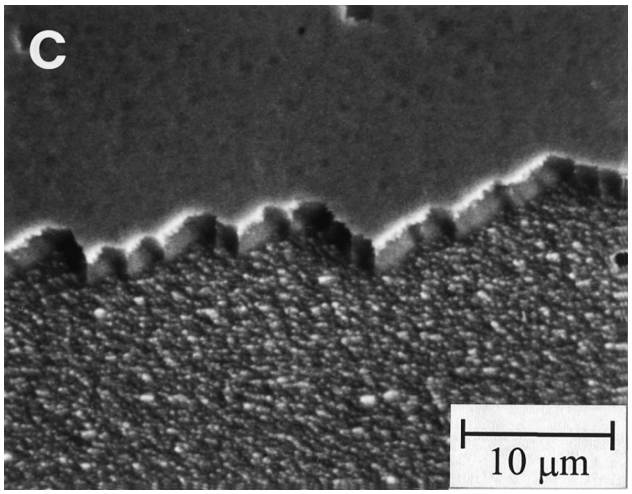

Fig. 5—The optical micrograph (*a*) of the 5 pct/800 °C/24 h specimen with grain boundaries faceted at large scales numbered from 1 to 6 and the SEM micrographs (*b*) and (*c*) of the grain boundaries 1 and 3.

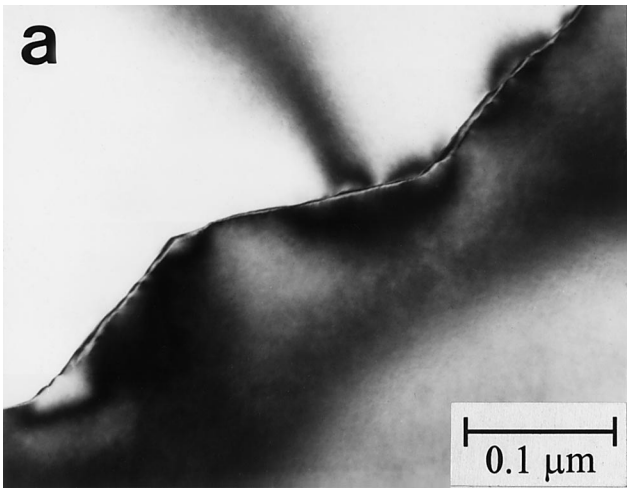

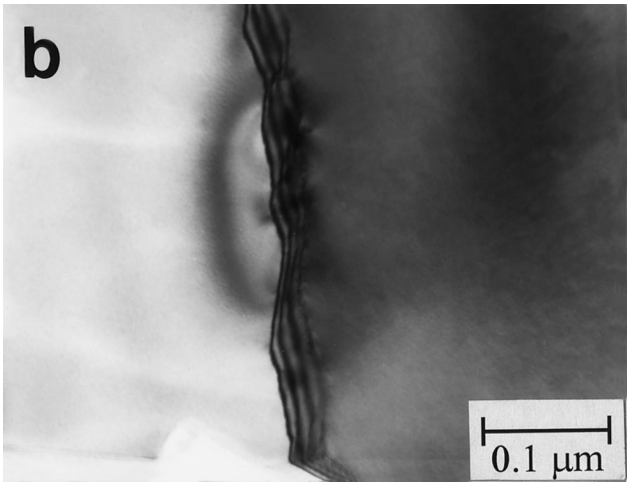

Fig. 6—(*a*) and (*b*) The TEM micrographs of the faceted grain boundaries observed in the 50 pct/800 °C/1 min specimen.

exhibited in Figure 6. These faceted shapes of the grain boundaries resembled those observed previously in other metals.[8,12,33] Most of the grain boundaries in the specimens annealed at temperatures lower than 800 °C were also found to be faceted, as will be described later, but with increasing annealing temperature, the fraction of the faceted grain boundaries decreased while the fraction of the smoothly curved boundaries increased. The details of this dependence on annealing temperature will be described later in this report. In general, the sizes of the faceted segments appeared to increase with the heat-treatment time and, hence, the grain size.

The faceted grain boundaries in these Cu specimens are similar to those observed in Ni,[8] Ag,[11] a Ni-based superalloy,[12] a stainless steel,[13] $BaTiO_3$,[15,34] and Al_2O_3.[16] As explained earlier,[8,11,12,16,17] at least some facet planes of faceted general grain boundaries are likely to be singular, with atomically flat structures corresponding to the cusps in the polar plot of the grain-boundary energy (γ) *vs* the grain-boundary normal or the inclination angle. The faceting of general grain boundaries has important implications on their atomic structure, because it means that the grain-boundary energy is critically dependent on the boundary normal. These faceted grain boundaries can move by two-dimensional nucleation of steps or on existing steps produced by dislocations, as proposed by Gleiter.[35,36,37] As proposed earlier[8,11,12,16,17] and illustrated in Figure 7, the grain-boundary migration rate will then increase nonlinearly with the driving force, causing rapid growth of only large grains and, hence, AGG. Such nonlinear variations of the migration rate with the driving force arising from boundary curvature were,

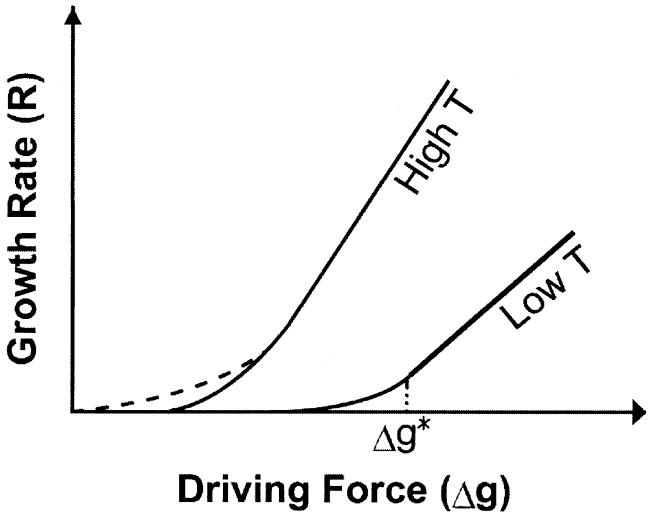

Fig. 7—Schematic variation of the rate of grain growth by two-dimensional nucleation with the driving force at high and low temperatures with the dashed curve for the dislocation growth mechanism at high temperature.

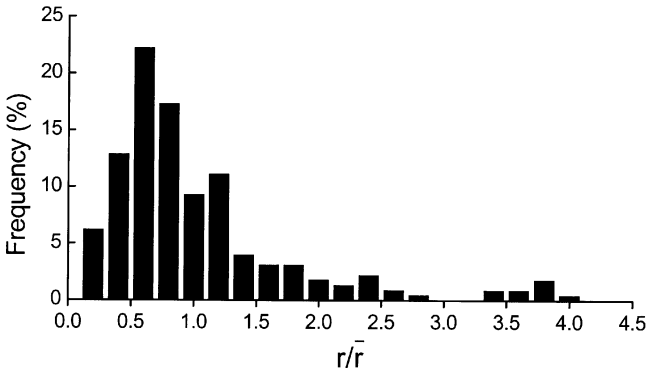

Fig. 8—The measured grain size distribution of the specimen shown in Fig. 4(c).

indeed, observed in bicrystals of Al[38] and an Fe-3 pct Si alloy.[39] If the grain boundaries have an atomically rough structure, the migration rate will increase linearly with the driving force. Then, normal grain growth will occur. In Ni,[8] Ag,[11] a Ni-based superalloy,[12] and a stainless steel,[13] the grain boundaries were observed to become defaceted and, therefore, atomically rough at high temperatures close to the melting points, and normal growth behaviors were, indeed, observed.

If the faceted grain boundaries migrate by growth on the steps produced by dislocations, the migration rate at low driving forces will be substantially higher than that by two-dimensional nucleation, as shown by a dashed curve in Figure 7. But at high driving forces, the growth can still occur by two-dimensional nucleation, and, with either type of nonlinear migration behavior with driving force shown in Figure 7, AGG can occur in the system of many grains. The two-dimensional nucleation model will be used for qualitative discussions in this report.

The observed dependence of AGG on initial grain size (which is determined by the deformation, as shown in Figure 3) and on annealing temperature appears to be consistent with this step-growth mechanism. We first examine the dependence on initial grain size. One characteristic of AGG is that it often appears to occur suddenly during the annealing treatment, as if there is an incubation time. After the primary recrystallization is completed, the grains undergo some coarsening before distinct AGG occurs. With still relatively narrow grain-size distributions, this stage of growth may appear to resemble normal growth, but because this type of growth was believed to occur also by a step mechanism, Yoon *et al.*[17] proposed to call it "stagnant growth." The duration of this stagnant growth corresponds to the incubation time for AGG.

In the 10 pct/800 °C series shown in Figure 4, for example, the stagnant growth appeared to occur during annealing for 2 hours (Figure 4(c)). The grain-size distribution of the 10 pct/800 °C/2 h specimen shown in Figure 4(c) was determined over a wide specimen area, carefully distinguishing the twin boundaries from the grain boundaries. This grain-size distribution with some large grains was wider than those observed for normal grain growth in Al.[40] In this stage of growth, it thus appeared that some grains began to grow slightly faster than the average and at some point began to accelerate to produce the distinct AGG structures. Therefore, experimentally, the duration of the stagnant growth or, equally, the incubation time for AGG could not be determined unambiguously. Hence, the period exactly between the completion of the primary recrystallization and the first distinct appearance of AGG was chosen as the incubation time for AGG. Figure 4 was selected as an example, because the duration of the stagnant growth and, therefore, the apparent incubation period was fairly long. As pointed out earlier, the primary recrystallization appeared to be complete after 15 minutes (Figure 4(a)), with an average grain size smaller than the initial value, and, hence, the period for the primary recrystallization was likely to be shorter than 15 minutes. It is also possible that the transition from the stagnant growth to AGG is actually quite gradual. Then, the incubation time for AGG will be inherently ambiguous and will only roughly indicate the first appearance of distinct AGG at various stages of the observation. Even when there is no primary recrystallization with very low or even no deformation, there can still be stagnant growth and, eventually, AGG, depending on the initial grain size and the heat-treatment temperature. Therefore, the apparent incubation time for AGG is generally meaningful with or without the primary recrystallization. The AGG behavior in Cu at low deformations will be examined in our next article.

As can be seen in the micrographs of Figures 2 and 4 and as shown in Figure 9, the incubation time was observed to decrease sharply with increasing deformation or decreasing initial grain size. The stagnant growth leading to AGG after a certain incubation time, which decreases with decreasing initial grain size, appears to be consistent with the step-growth mechanism. In the theory of growth by two-dimensional nucleation of boundary steps,[17,41] the growth rate (R) depends on the step-edge free energy ($\sigma(T)$) and the driving force (Δg) as

$$R \propto \exp\left(\frac{-\pi V_m \sigma(T)^2}{h \Delta g k T}\right) \qquad [1]$$

where V_m is the molar volume, h is the step height, k is the Boltzmann constant, and T is the temperature. As in most of the grain-growth theories, it may be assumed that Δg is approximately given as

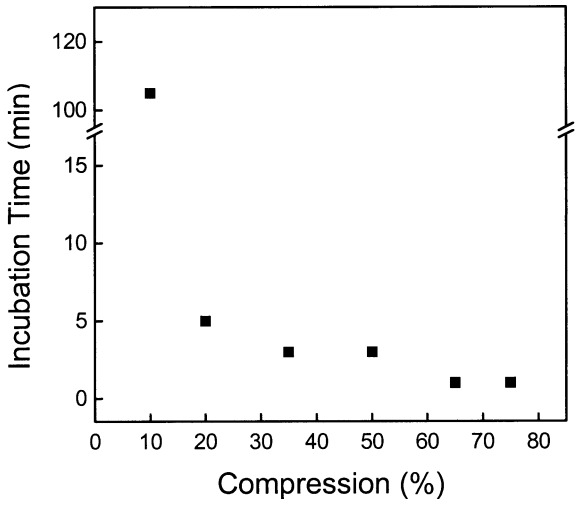

Fig. 9—The variation of the incubation time for AGG with the level of compression in the specimens annealed at 800 °C.

$$\Delta g_i(\bar{r}, r_i) = \beta V_m \gamma \left(\frac{1}{\bar{r}} - \frac{1}{r_i} \right) \quad [2]$$

where β is a geometric factor, γ is the grain-boundary energy, r_i is the size of the growing grain, and $\bar{r}$ is the average size of the grains surrounding it, which may be assumed to be the average size of all grains. For a large grain growing abnormally in the matrix of fine grains, $\bar{r}$ will represent the average size of the matrix grains. Writing $r_i = \alpha_i \bar{r}$,

$$\Delta g_i(\bar{r}, r_i) = \frac{\beta V_m \gamma}{r} \left(\frac{\alpha_i - 1}{\alpha_i} \right) \quad [3]$$

Because the driving force for the growth of a grain of size r_i depends on both $\bar{r}$ and α_i (equal to $r_i/\bar{r}$), the size of the large grains relative to $\bar{r}$ (or α_i) must be large enough to exceed the critical driving force (Δg^*). The Eq. [1] for R as a function of Δg is schematically shown in Figure 7 at two temperatures. Because this equation describes the growth by mononucleation, it is expected to be valid at relatively low driving forces. As the driving force increases, polynucleation is expected to occur with a slightly different dependence on Δg, and above Δg^*, R is expected to increase linearly with Δg, as shown in Figure 7, because the growth will be limited by the rate the of atom jump across the boundary.

It appears that initially (at the completion of the primary recrystallization), none of the large grains has a large enough size to exceed Δg^*, which is required for AGG. Then, all grains will grow at very low rates in the low-driving-force range shown in Figure 7. Such a slow growth limited by the nucleation of steps is the stagnant growth. During the stagnant growth, large grains can grow relatively faster than the increase of the average size because of the nonlinear variation of the growth rate with the driving force, and when the large grains attain the critical sizes required to exceed Δg^*, they will undergo accelerated growth to produce AGG. If the initial $\bar{r}$ value is smaller, the time required for the large grains to exceed Δg^* will be shorter. Therefore, the incubation time will decrease with decreasing initial grain size, in agreement with the experimental results shown in Figure 9.

If at any stage of the stagnant growth $\bar{r}$ becomes larger than $\beta V_m \gamma / \Delta g^*$, even a grain of infinitely large size cannot grow abnormally. Then, AGG will never occur and the stagnant growth will persist indefinitely during the annealing treatment. In the 5 pct/800 °C series shown in Figure 10, the stagnant growth appeared to persist during annealing for 100 hours, and it is possible that even during further annealing, AGG will not occur. In such a specimen, even a grain of very large size, which may be produced artificially by, for example, diffusion bonding a large single crystal, may not grow at a high rate. Therefore, it appears that there is a maximum limit to the initial grain size for AGG.

The possibly persistent stagnant growth shown in Figure 10 (for the specimen deformed to 5 pct) or the stagnant growth during a relatively long period (2 hours), shown in Figure 4 (for the specimen deformed to 10 pct), before the occurrence of AGG may appear to resemble normal growth, but their mechanisms are fundamentally different. The stagnant growth occurs because none of the large grains, often because of the large matrix grain size or the low temperature, are exposed to a sufficiently large capillary driving force to exceed Δg^*, as shown in Figure 7. Then, even the large grains will grow slowly, limited by the step nucleation or movement, although they will grow relatively faster than the smaller grains. If some grains during the stagnant growth become large enough to exceed Δg^*, they will grow rapidly with kinetic roughening of the grain boundaries, producing the AGG behavior. In normal grain growth, the grain boundaries are thermodynamically rough, with abundant thermally induced steps. Therefore, all grains can rapidly grow without any limitation of the boundary step process. The stagnant, abnormal, and normal growths are, thus, critically dependent on the thermodynamic and kinetic roughening of the grain boundaries.

The number of abnormally large grains in the early stages of AGG and their sizes after their impingement were also found to depend on the level of deformation. In Figure 2, for the 50 pct/800 °C series, for example, some grains grew to large sizes after annealing for 4 minutes (Figure 2(b)) and began to impinge upon each other after 10 minutes (Figure 2(c)). The impingement appeared to be almost complete after 24 hours (Figure 2(d)) with the disappearance of most of the fine grains. Because most of the large grains were formed at the early stages of AGG and grew until they impinged upon each other, the grain sizes after the impingement decreased with increasing number density of the abnormal grains in the early stage. As shown in Figures 2 and 4, the number of abnormal grains increased with increasing deformation, and, therefore, the size of the impinged grains decreased, as shown in Figures 11 and 12. Figure 11 shows the microstructures of the specimens compressed to various levels and annealed at 800 °C until the abnormally large grains impinged upon each other, and their average sizes at various compressions are shown in Figure 12. (Figure 11(c) is same as Figure 2(c), but is shown again to facilitate the comparison.) In the specimens compressed to 20 and 10 pct, there were only 5 and 3 large impinged grains, respectively, at the specimen cross sections, and their average sizes are shown in Figure 12. In the specimens compressed to 35, 50, 65, and 75 pct, the ten largest grains were selected to obtain the average values which are also shown in Figure 12. Although the number of grains that were used to estimate the average sizes was small because of

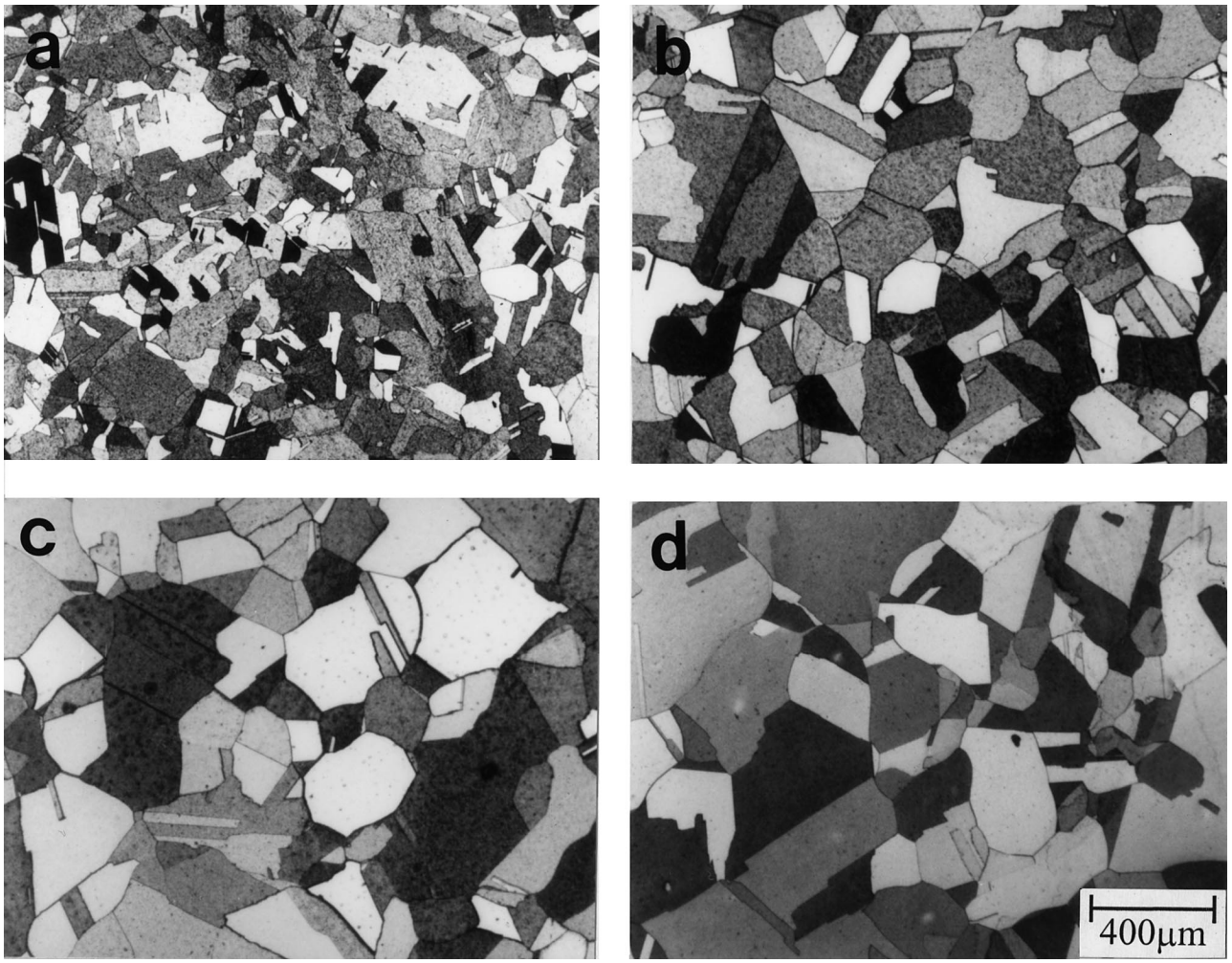

Fig. 10—The optical microstructures of the specimens annealed at 800 °C for (*a*) 5 min, (*b*) 1 h, (*c*) 24 h, and (*d*) 100 h after 5 pct compression.

the limited total numbers at low deformations, Figure 12 roughly shows the large variation of the impinged abnormal grain size with compression, which is also evident in Figure 11. The observed variation of the number density and, hence, the impinged size of the abnormal grains with the level of deformation can also be explained in terms of Eq. [3]. The number of grains with large enough relative sizes during the stagnant growth to exceed Δg^* will increase with the decreasing average grain size $\bar{r}$ for the same normalized size distribution (or the same α_i), according to Eq. [3]. Furthermore, the probability of producing an abnormal grain per unit volume of the specimen will increase with the increasing number density of the grains.

After the large grains impinge upon each other, they usually undergo slow stagnant growth indefinitely. The 50 pct/800 °C series shown in Figure 2 appeared to be such a case, as well as the specimens deformed to lower levels. But in the specimens compressed to 65 and 75 pct, AGG occurred again during further annealing after the impingement, as shown in Figure 13 for the 65 pct/800 °C series. The first AGG occurred after annealing for 2 minutes (Figure 13(b)), the impingement occurred after 10 minutes (Figure 13(c)), and AGG occurred again, resulting in very large grains after 24 hours (Figure 13(d)). A similar double AGG behavior was observed in the 75 pct/800 °C series. Such double AGG occurred in these specimens, apparently because the grain sizes after the first impingement were 198 and 168 μm, respectively, for the 65 pct/800 °C and 75 pct/800 °C series, which were smaller than the grain size of 244 μm for the 5 pct/800 °C/1 h specimen (Figure 10(b)), which showed, apparently, a persistent stagnant growth behavior during annealing for 100 hours. In contrast, the 50 pct/800 °C series showed an impinged grain size of 657 μm, which was larger than 244 μm. Therefore, this specimen was, indeed, expected to show persistent stagnant growth after the impingement, without a double AGG behavior. Therefore, the double AGG behavior is consistent with the maximum limit of the initial grain size for AGG. Previously, the AGG behaviors in polycrystals were apparently not examined completely enough to discover the double AGG behavior.

The annealing treatments of the deformed specimens were also carried out at 600 °C, 700 °C, 900 °C, 950 °C, and 1050 °C. The grain sizes after primary recrystallization appeared to be independent of the annealing temperature, in agreement with the previous observations of Eastwood *et al.* in α-brass[21] and Al.[22] Therefore, the initial grain sizes for grain growth in the specimens deformed to various levels and annealed at different temperatures are approximately the same as those shown in Figure 3 for the annealing temperature of 800 °C. The times required to complete the primary

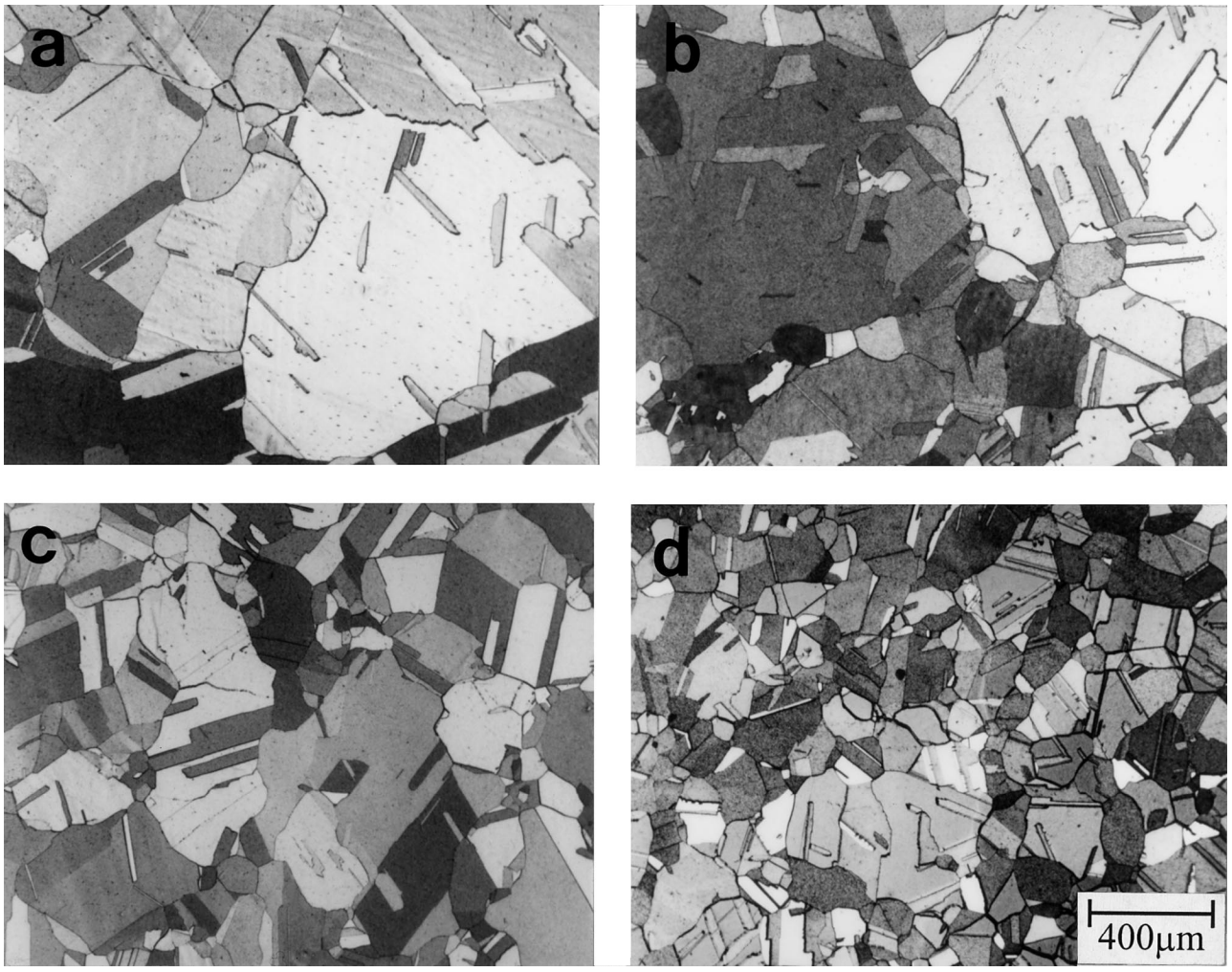

Fig. 11—The optical microstructures of the specimens annealed at 800 °C (*a*) for 20 min after 20 pct compression, (*b*) for 10 min after 35 pct compression, (*c*) for 10 min after 50 pct compression, and (*d*) for 10 min after 75 pct compression.

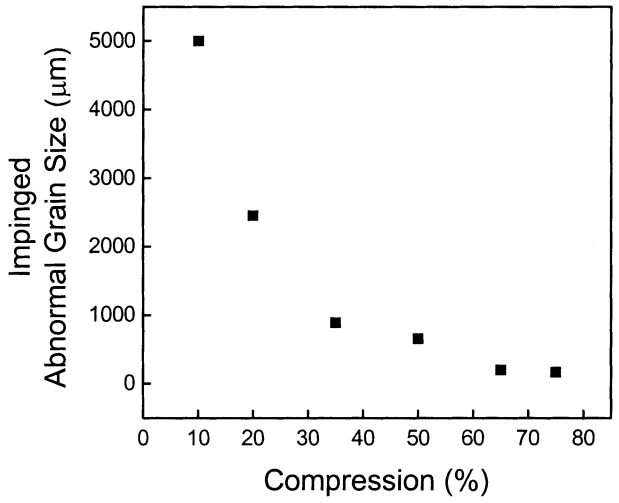

Fig. 12—The average sizes of the impinged abnormal grains in the specimens annealed at 800 °C after compressing to various levels.

recrystallization were shorter at higher temperatures. The grain growth in the 50 pct/1050 °C series is shown in Figure 14. The primary recrystallization appeared to be complete after 30 seconds (Figure 14(a)), and the subsequent grain growth (up to 2 hours) appeared to be almost normal, without any pronounced AGG. In contrast, the 20 pct/1050 °C/3 min specimen showed a distinct AGG.

When examined under SEM, most of the grain boundaries in the 50 pct/1050 °C/2 min specimen (Figure 14(d)) were found to be smoothly curved (defaceted), as shown in Figure 15, in contrast to the faceted grain boundaries in the 5 pct/800 °C/24 h and 50 pct/800 °C/1 min specimens, shown in Figures 5 and 6, respectively. It, thus, appeared that most of the grain boundaries underwent defaceting transitions at temperatures between 800 °C and 1050 °C and became rough. Such a defaceting transition of general grain boundaries is similar to that observed in Ni[8] and a Ni-based superalloy.[12] But even at 1050 °C, which is fairly close to the melting point (1083 °C), some grain boundaries still remained faceted. Previously, it was also observed that in a carburizing atmosphere all grain boundaries in Ni became defaceted at 0.7 T_m, where T_m is the melting point, but in vacuum, some grain boundaries remained faceted even at 0.95 T_m. Therefore, in vacuum, most of the grain boundaries in both Cu and Ni became defaceted at temperatures close to their melting points, but a small fraction of them remained faceted.

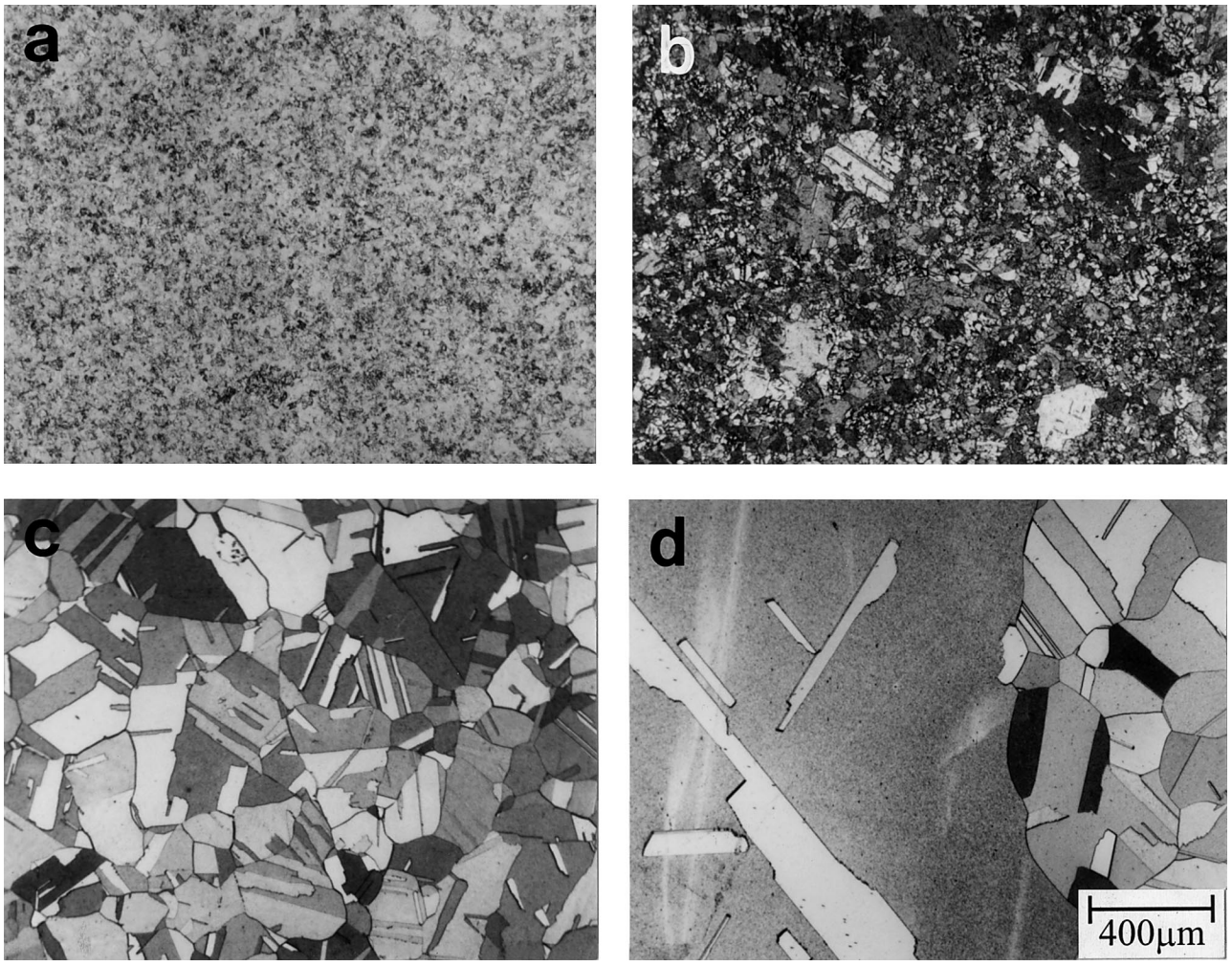

Fig. 13—The optical microstructures of the specimens annealed at 800 °C for (*a*) 1 min, (*b*) 2 min, (*c*) 10 min, and (*d*) 24 h after 65 pct compression.

As pointed out earlier by Yoon *et al.*[17] and Lee *et al.*,[8] the defaceting transition of grain boundaries is analogous to that of the crystal surface. The defaceting transition, which is usually a first-order transition,[14] normally implies roughening of the boundaries with singular orientations corresponding to the cusps in the polar plot of the boundary energy *vs* the inclination angle. If the roughening of singular grain boundaries is a higher-order transition analogous to the roughening of crystal surfaces, it can be represented by a gradually decreasing boundary step-edge free energy ($\sigma(T)$), with the increasing temperature becoming 0 at the roughening transition temperature.[42–46] Therefore, the R *vs* Δg curves will be strongly temperature dependent, as illustrated in Figure 7. The value of Δg^* will decrease with increasing temperature until it becomes 0 at the roughening transition temperature.

The dependence of AGG behavior on temperature can be readily predicted from the two-dimensional nucleation model, using Eqs. [1] and [3]. Combining these two equations, the growth rate (R_i) for a grain of size r_i will be

$$R_i \propto \exp\left(\frac{-\alpha_i \pi \sigma(T)^2 \bar{r}}{(\alpha_i - 1)\beta\gamma h\mathrm{k}T}\right) \qquad [4]$$

Therefore, the decrease of $\sigma(T)$ with increasing temperature will have the same effect as decreasing the initial average grain size. It is then expected that the incubation time for AGG will decrease, the number of the abnormal grains will increase, and, hence, the size of impinged grains will decrease with increasing annealing temperature. These predictions were found to qualitatively agree with the observations.

The incubation time for AGG was observed to decrease with increasing annealing temperature. For examples, in the specimens deformed to 20 pct, the earliest times for observing AGG were 3 minutes at 1050 °C, 10 minutes at 800 °C, and 1 hour at 700 °C. In the specimens deformed to 50 pct, the earliest times for AGG were 15 minutes at 600 °C, 15 minutes at 700 °C, 4 minutes at 800 °C (Figure 2(b)), and 1.5 minutes at 950 °C. These times only roughly represent the incubation times for AGG, because they are difficult to determine precisely. The 20 pct/600 °C series showed stagnant growth during annealing for 100 hours, and it is possible that even upon annealing for much longer periods, AGG will not occur as in the case of the 5 pct/800 °C series (Figure 10) discussed earlier. Because Δg^* is larger at lower temperatures, the maximum average size for AGG ($\bar{r}^*$) is smaller. Therefore, although the specimens deformed to 20 pct have a smaller grain size after recrystallization than those deformed to 5 pct, they can undergo persistent stagnant growth at low temperatures. Such a behavior indicates that

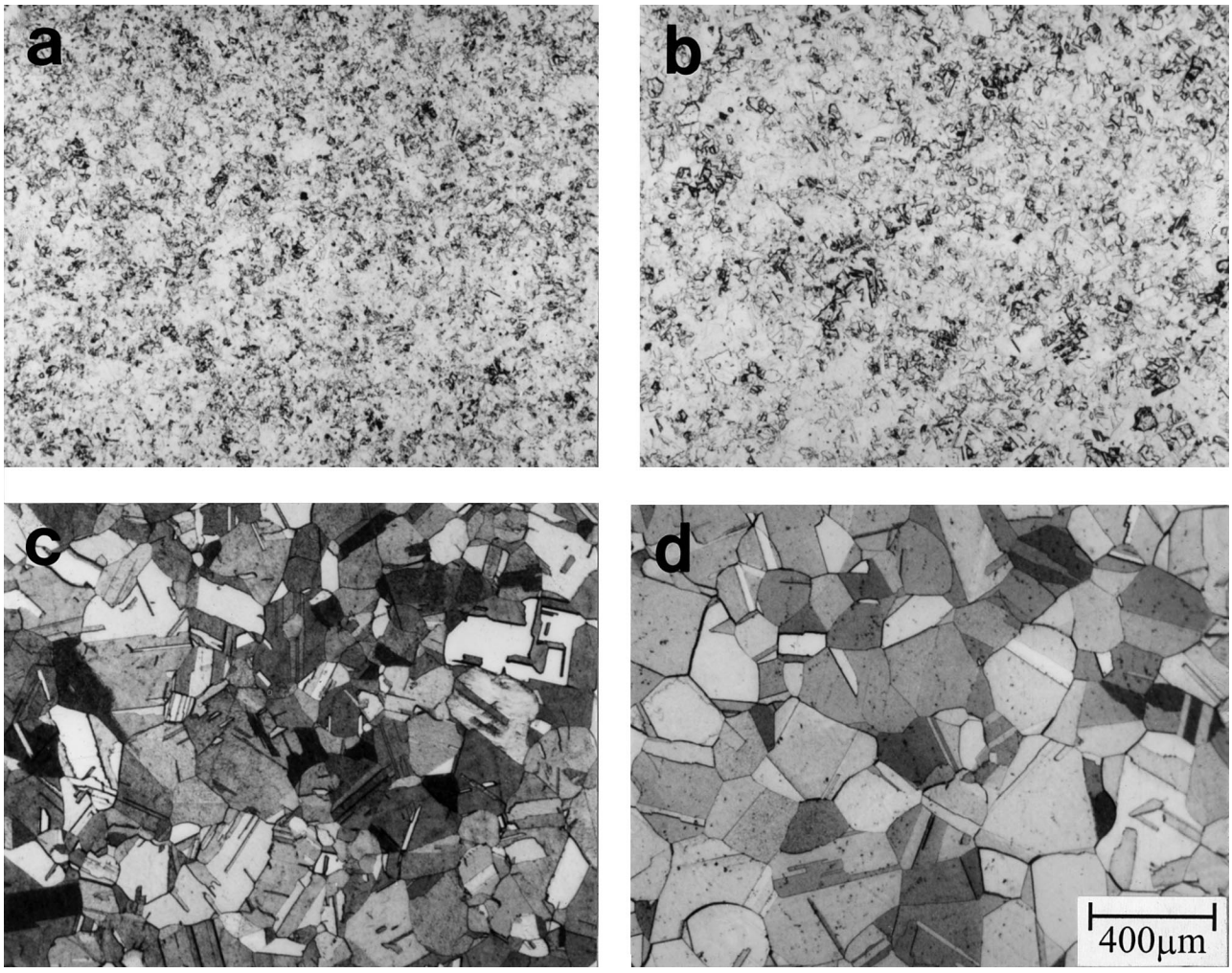

Fig. 14—The optical microstructures of the specimens annealed at 1050 °C for (*a*) 30 s, (*b*) 40 s, (*c*) 1.5 min, and (*d*) 2 min after 50 pct compression.

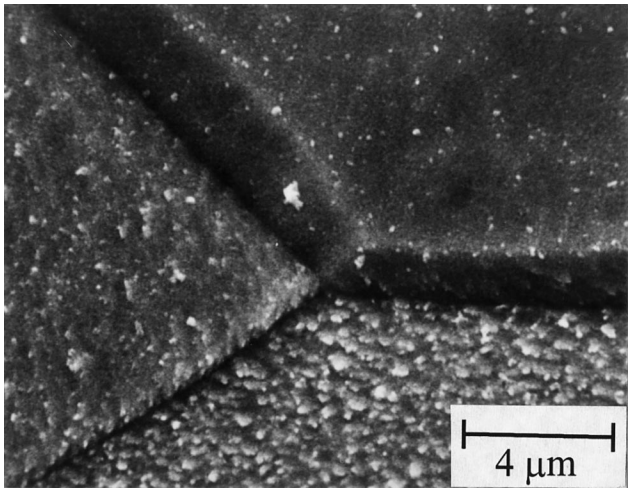

Fig. 15—The SEM micrograph of the defaceted grain boundaries in the 50 pct/1050 °C/2 min specimen.

there is a lowest temperature required for AGG for a given initial grain size or deformation. This lowest temperature for AGG increases with increasing initial grain size.

For the same deformation, the number density of abnormally large grains decreased with decreasing temperature. The microstructural evolution during annealing for the 50 pct/600 °C series is shown in Figure 16 as an example. The abnormal grains appeared after annealing for 15 minutes (Figure 16(b)), and their number density was smaller (and, hence, their sizes larger) than the abnormal grains observed in the 50 pct/800 °C/4 min specimen (Figure 2(b)). The impinged abnormal grains were, therefore, larger at 600 °C (Figure 16(d)) than those at 800 °C (Figure 2(c)). As shown in Figures 17 and 18, the impingement of the abnormal grains generally occurred later, and their average sizes were larger at lower temperatures.

As pointed out earlier, this observation is consistent with Eq. [4], which shows that decreasing $\sigma(T)$ (with increasing temperature) has the same effect as decreasing $\bar{r}$ on AGG, but it should be noted that the change of $\sigma(T)$ affects the probability of AGG per grain, while the change of $\bar{r}$ can affect both the probabilities of AGG per unit volume as well as per grain. As pointed out earlier, the grain size at the completion of primary recrystallization appeared to be independent of the annealing temperature, and, hence, the initial grain sizes for AGG at different annealing temperatures were approximately the same if the deformation levels were the same. In order to confirm that the variation of the impinged grain size with the annealing temperature shown in Figure 17 was not caused by any variation of the initial grain size,

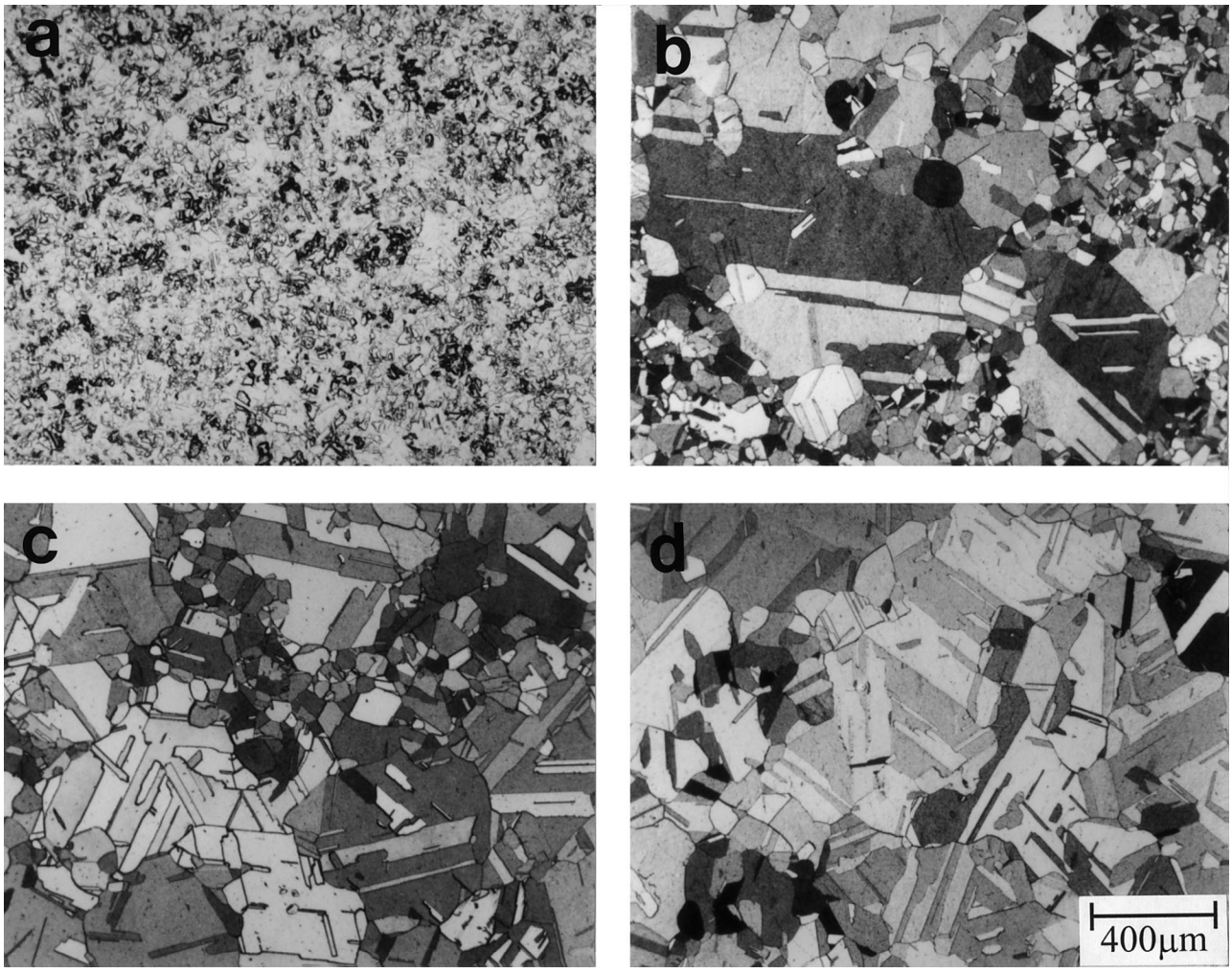

Fig. 16—The optical microstructures of the specimens annealed at 600 °C for (*a*) 3 min, (*b*) 15 min, (*c*) 30 min, and (*d*) 2 h after 50 pct compression.

some specimens deformed to 50 pct were initially recrystallized at 800 °C for 1 minute to obtain the structure shown in Figure 2(a) and were separately annealed further at 600 °C, 700 °C, 800 °C, and 950 °C. The impinged grain sizes were approximately the same as those in Figures 17 and 18.

As pointed out earlier, all specimens heat treated at low temperatures showed many faceted grain boundaries. Figure 19 shows the SEM micrographs of the faceted grain boundaries in the 50 pct/600 °C/30 min specimen (Figure 16(c)). As shown in Figure 16, AGG appeared to be nearly complete in this specimen and most of the grain boundaries were faceted, as shown in Figure 19.

As the temperature exceeds or approaches the roughening temperatures of the grain boundaries, most of the grains can grow at high rates approaching the continuous growth rate. Then, the growth behavior can approach that of normal growth. The growth behavior observed in the 50 pct/1050 °C series shown in Figure 14 appears to be such a case. Because of the rapid grain growth, it could not be clearly determined if AGG occurred between the heat-treatment periods of 30 and 40 seconds (Figures 14(a) and (b)), but the growth after 90 seconds, shown in Figures 14(c) and (d), appeared to be normal. If the annealing temperature can be further increased until all grain boundaries become rough, they will grow normally because all of them can grow continuously. During annealing at 1050 °C, distinct AGG was still observed when the recrystallized grain size was larger with a 20 pct deformation, because with some grain boundaries still remaining faceted, distinct AGG can still occur with a relatively large initial grain size.

When the 50 pct/950 °C/6 min specimen (shown in Figure 20(c)) with impinged abnormal grains was further annealed for 10 hours (Figure 20(d)), the grains showed a double AGG behavior producing very large grains. In contrast, the 50 pct/800 °C series (Figure 2) did not show such a double AGG behavior, because the impinged grains were large. The 65 pct/800 °C (Figure 13) and 75 pct/800 °C series, on the other hand, showed double AGG, because the impinged grains were smaller than those in the 50 pct/800 °C series. Summarizing the grain-growth behavior of the specimens deformed to 50 pct, AGG occurred at 600 °C, 700 °C, and 800 °C, double AGG occurred at 900 °C and 950 °C, and nearly normal growth occurred at 1050 °C.

The observed variation of the grain-growth behavior with deformation and annealing temperature is summarized in Figure 21. The stagnant growth behaviors were observed to be persistent during annealing for 100 hours and are likely to last for much longer periods. The nearly normal growth

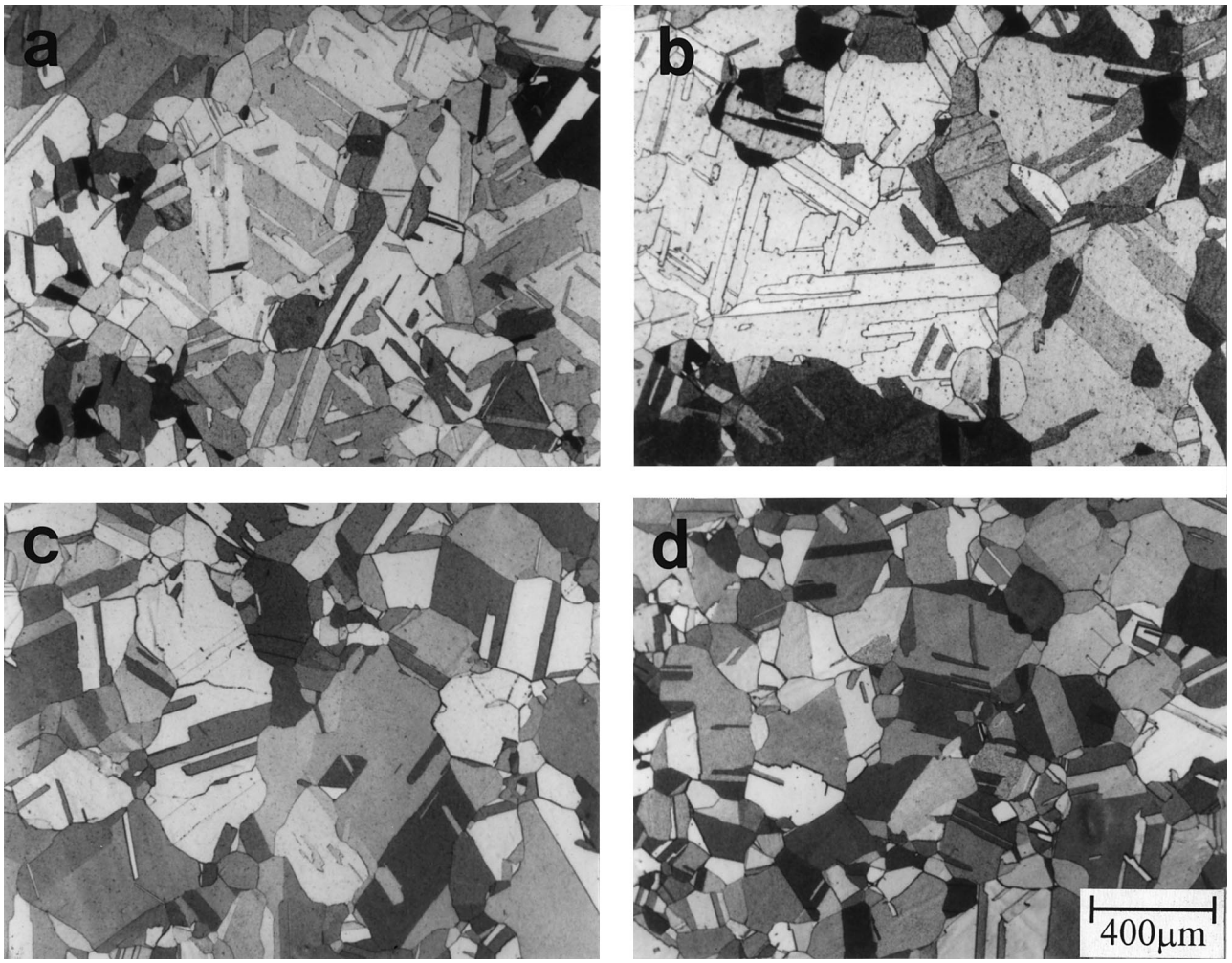

Fig. 17—The optical microstructures of the specimens annealed at (*a*) 600 °C for 2 h, (*b*) 700 °C for 1 h, (*c*) 800 °C for 10 min, and (*d*) 950 °C for 6 min after 50 pct compression.

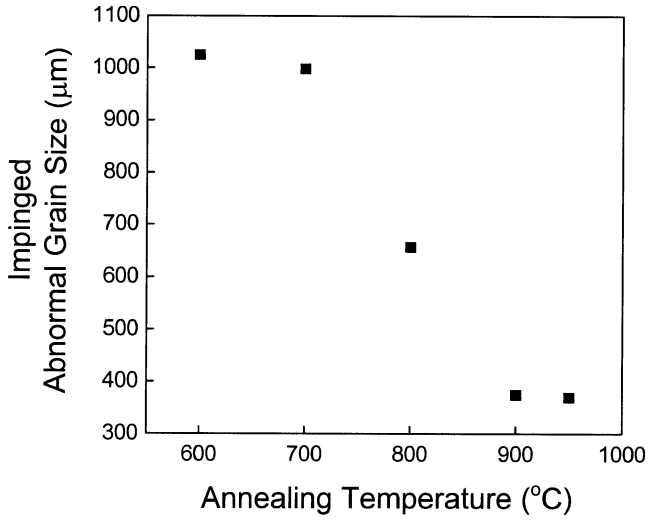

Fig. 18—The average sizes of the impinged abnormal grains in the specimens compressed to 50 pct and annealed at various temperatures.

in the 50 pct/1050 °C series (indicated by Δ) deviates from the pattern because, with the grain boundaries mostly rough and with a relatively fine initial grain size, the growth at this temperature resembled normal growth. This result confirms the earlier proposal[8,11,17] that the normal growth is actually a limit of AGG when all grain boundaries become rough and, hence, can move continuously without producing the boundary steps. Or, the rough grain boundaries can be viewed as having an infinite number of thermally activated boundary steps.

Previously, the kinetics of AGG has been often analyzed with the Johnson–Mehl–Avrami equation[47–50] for the nucleation and growth process. But, because the fine matrix grains also undergo stagnant growth during AGG, as can be seen, for example, in Figures 2, 13, 16, and 20, it is not quite correct to apply this equation assuming that the matrix remains constant during AGG.

IV. CONCLUSIONS

The observation of the faceted grain boundaries in pure Cu indicates, as in other pure metals[8,11] and single-phase alloys,[12,13] that AGG occurs by the boundary step mechanism. The fine matrix grains undergo stagnant growth limited by the slow rates of step production at low driving forces, and the stagnant growth may persist forever at low temperatures with a large initial grain size. The incubation time for

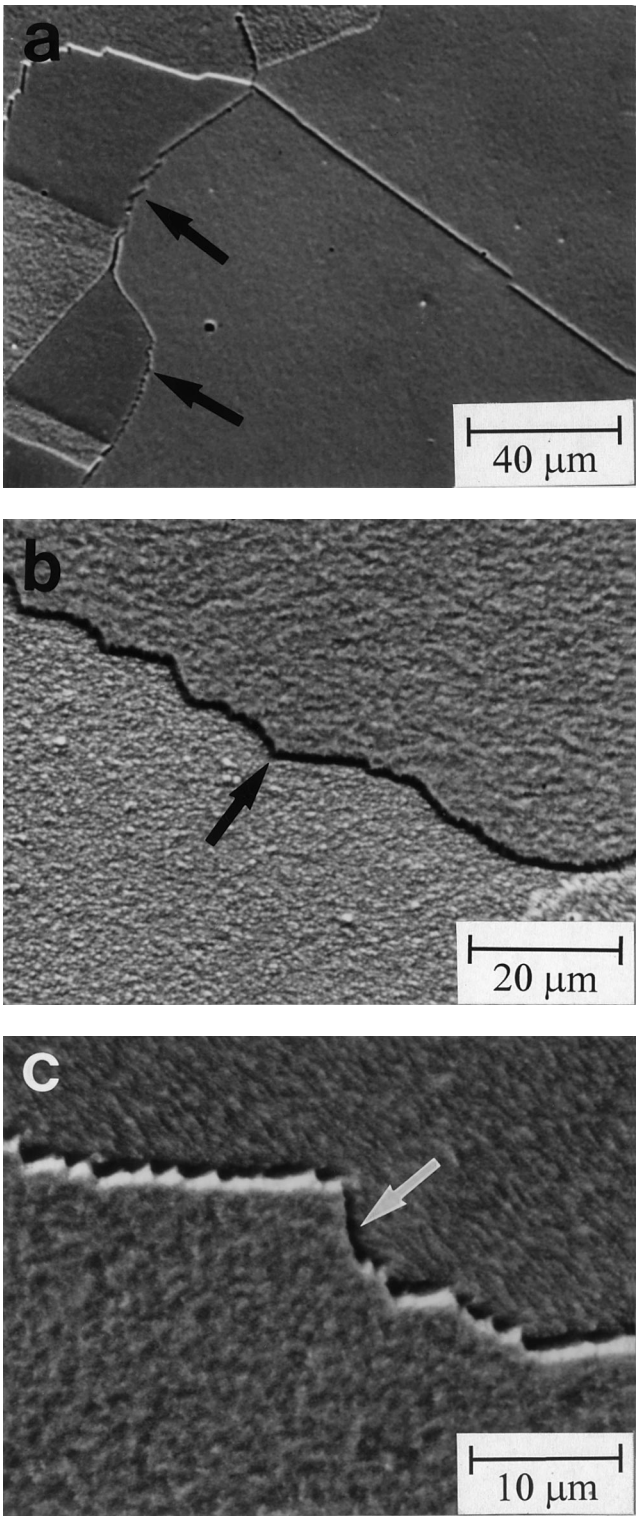

Fig. 19—(*a*) through (*c*) The SEM micrographs of the faceted grain boundaries (indicated by arrows) observed in the 50 pct/600 °C/30 min specimen (shown in Fig. 16(c)).

AGG decreases and the number density of abnormally large grains increases with decreasing initial grain size and increasing annealing temperature. At high temperatures with a small initial grain size, double AGG occurs. These observations are qualitatively consistent with and, therefore, provide indirect evidence for the step-growth mechanism by two-dimensional nucleation. Even with dislocations essentially the same, the step-growth mechanism can apply with similar effects of the step-edge free-energy change with temperature and matrix grain size. A better understanding of the migration mechanism of the faceted grain boundaries is needed. Although the grain-size distributions were determined for some of the specimens, they often are not more revealing than direct observations of the microstructures, because there are expected to be inherent ambiguities in distinguishing among the stagnant, abnormal, and normal growth modes, according to the step-growth model. Each growth mode is a limiting case of the other and, hence, often is not clearly distinguishable from it. Numerical solutions and modeling of the growth behavior with the step-growth mechanism will be useful for quantitative analysis of the observations.

In this work, all specimens were first compressed to 30 pct and annealed at 500 °C for 30 minutes in order to fix the initial grain size before the subsequent compression and annealing treatments. If this initial grain size is varied, the AGG behavior will also change at low deformations, because the recrystallized grain size will generally be larger with a larger initial grain size at low deformations.[6,51,52] But at high deformations, the recrystallized grain size and, hence, AGG behavior will be nearly independent of the initial grain size. For the specimens deformed to 5 and 10 pct in this work, it is possible that primary recrystallization did not occur at temperatures below 800 °C and, hence, there was no decrease of the grain size from the initial value. But the results are still significant for showing the variation of the AGG behavior with the initial grain size. In order to avoid the effect of remaining strain, the initial grain size has to be now defined more carefully as the stage when the grains have grown sufficiently to be free of any strain. The effect of low strains at the levels below those required for primary recrystallization will be described in our next article.

ACKNOWLEDGMENTS

This work was supported by the Corporate Research and Development Center, General Electric Company, and by the Korea Ministry of Education through the Brain Korea 21 Program. Discussions with M.F. Henry were greatly helpful.

REFERENCES

1. C.G. Dunn and J.L. Walter: in *Recrystallization, Grain Growth and Textures*, H. Margolin, ed., ASM, Metals Park, OH, 1966, pp. 461-521.
2. G. Riontino, C. Antonione, L. Battezzati, F. Marino, and M.C. Tabasso: *J. Mater. Sci.*, 1979, vol. 14, pp. 86-90.
3. C.J. Simpson, K.T. Aust, and W.C. Winegard: *Metall. Trans.*, 1971, vol. 2, pp. 987-91.
4. W.A. Miller and W.M. Williams: *J. Inst. Met.*, 1964, vol. 93, pp. 125-27.
5. M.L. Kronberg and F.H. Wilson: *Trans. TMS-AIME*, 1949, vol. 185, pp. 501-14.
6. M. Çigdem: *Z. Metallkd.*, 1994, vol. 85, pp. 723-32.
7. V. Randle and D. Horton: *Scripta Metall. Mater.*, 1994, vol. 31, pp. 891-95.
8. S.B. Lee, N.M. Hwang, D.Y. Yoon, and M.F. Henry: *Metall. Mater. Trans. A*, 2000, vol. 31A, pp. 985-94.
9. F.D. Rosi, B.H. Alexander, and C.A. Dube: *Trans. TMS-AIME*, 1952, vol. 152, pp. 189-96.
10. J.S. Bowles and W. Boas: *J. Inst. Met.*, 1948, vol. 74, pp. 501-19.
11. J.B. Koo and D.Y. Yoon: *Metall. Mater. Trans. A*, 2001, vol. 32A, pp. 469-75.

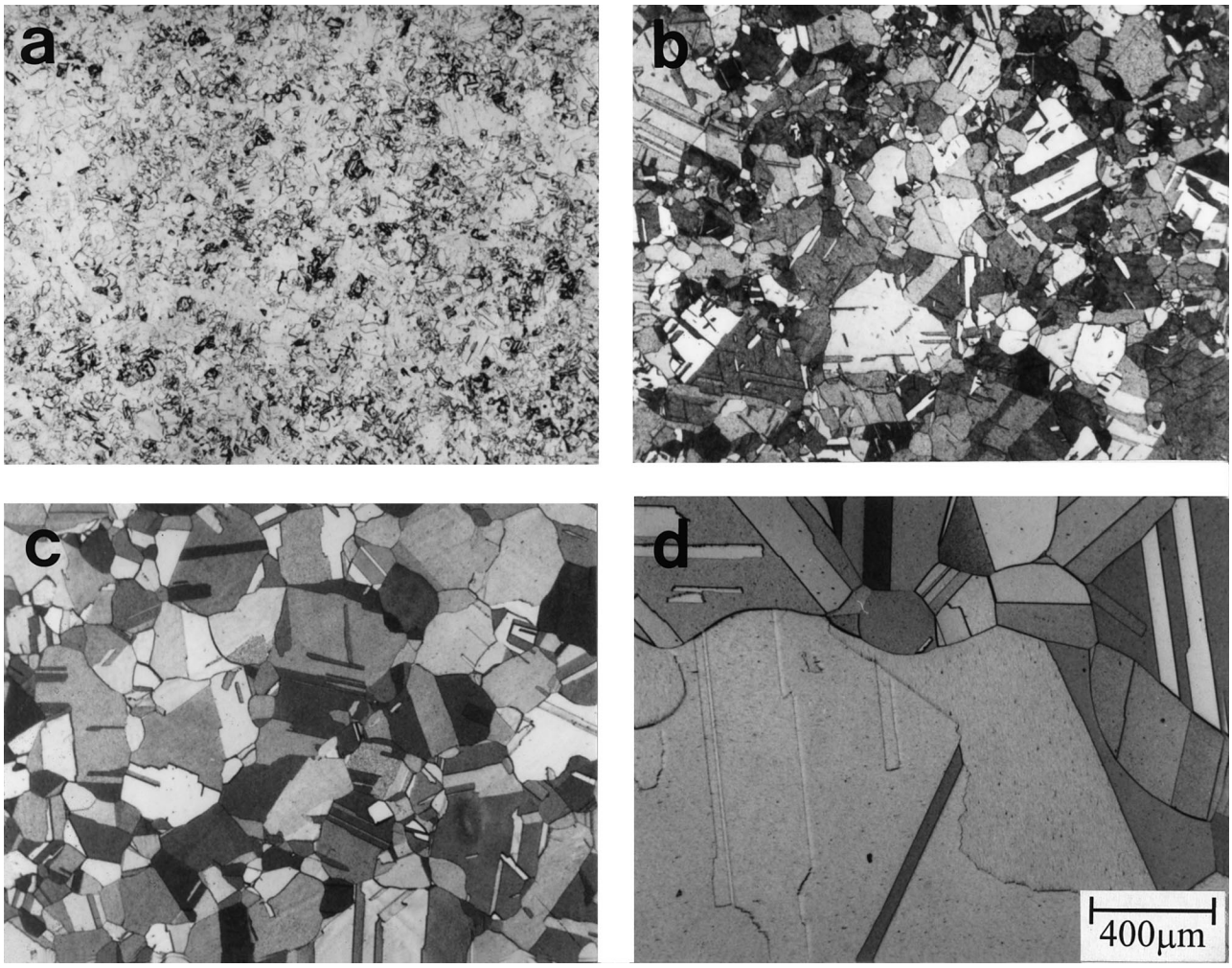

Fig. 20—The optical microstructures of the specimens annealed at 950 °C for (*a*) 1 min, (*b*) 1.5 min, (*c*) 6 min, and (*d*) 10 h after 50 pct compression.

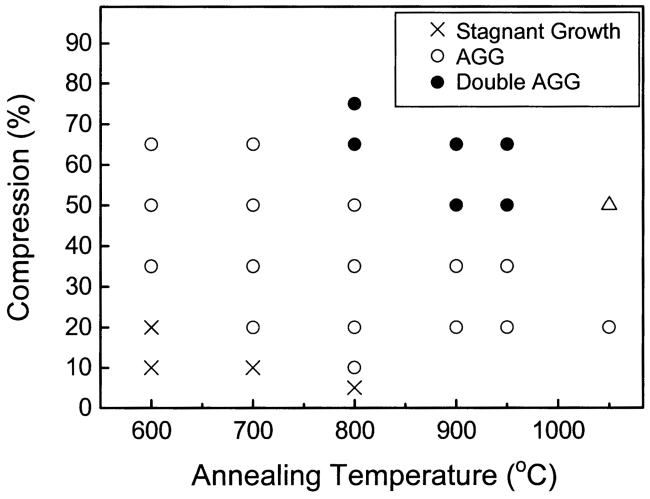

Fig. 21—The dependence of grain growth behavior on deformation and annealing temperature.

12. S.B. Lee, D.Y. Yoon, and M.F. Henry: *Acta Mater.*, 2000, vol. 48, pp. 3071-80.
13. J.S. Choi: Masters Thesis, Korea Advanced Institute of Science and Technology, Taejon, Korea, 1997.
14. J.W. Cahn: *J. Phys. Colloq. 6*, 1982, No. 12, pp. 199-213.
15. B.K. Lee, S.Y. Chung, and S.J.L. Kang: *Acta Mater.*, 2000, vol. 48, pp. 1575-80.
16. C.W. Park and D.Y. Yoon: *J. Am. Ceram. Soc.*, 2000, vol. 83, pp. 2605-09.
17. D.Y. Yoon, C.W. Park, and J.B. Koo: *Proc. Int. Workshop on Ceramic Interfaces: Properties and Application IV (Ceramic Interfaces 2)*, H.I. Yoo and S.J.L. Kang, eds., The Institute of Materials, London, 2001, pp. 3-21.
18. Y.J. Park, N.M. Hwang, and D.Y. Yoon: *Metall. Mater. Trans. A*, 1996, vol. 27A, pp. 2809-19.
19. P. Wynblatt and N.A. Gjostein: *Acta Metall.*, 1976, vol. 24, pp. 1165-74.
20. P. Wynblatt: *Acta Metall.*, 1976, vol. 24, pp. 1175-82.
21. L.W. Eastwood, A.E. Bousu, and C.T. Eddy: *Trans. TMS-AIME*, 1935, vol. 117, pp. 246-64.
22. L.W. Eastwood, R.W. James, and R.F. Bell: *Trans. TMS-AIME*, 1939, vol. 133, pp. 124-41.
23. W.A. Anderson and R.F. Mehl: *Trans. TMS-AIME*, 1945, vol. 161, pp. 140-72.
24. E.M. Zielinski, R.P. Vinci, and J.C. Bravman: *J. Appl. Phys.*, 1994, vol. 76, pp. 4516-23.
25. E.M. Zielinski, R.P. Vinci, and J.C. Bravman: *Appl. Phys. Lett.*, 1995, vol. 67, pp. 1078-80.
26. J. Zhang, K. Xu, and J. He: *J. Mater. Sci. Lett.*, 1999, vol. 18, pp. 471-73.
27. C. Antonione, G.D. Gatta, G. Riontino, and G. Venturello: *J. Mater. Sci.*, 1973, vol. 8, pp. 1-10.
28. C. Antonione, F. Marino, G. Riontino, and M.C. Tabasso: *J. Mater. Sci.*, 1977, vol. 12, pp. 747-50.

29. V. Randle and A. Brown: *Phil. Mag. A*, 1988, vol. 58, pp. 717-36.
30. J.S. Woo, J.C. Park, and K. Lee: *J. Kor. Inst. Met.*, 1982, vol. 20, pp. 914-21.
31. C.S. Barrett and T.B. Massalski: *Structure of Metals*, 3rd ed., Pergamon Press, Oxford, United Kingdom, 1980, pp. 541-83.
32. W.M. Baldwin: *Trans. TMS-AIME*, 1946, vol. 166, pp. 591-611.
33. T.E. Hsieh and R.W. Balluffi: *Acta Metall.*, 1989, vol. 37, pp. 2133-39.
34. T. Yamamoto, Y. Ikuhara, K. Hayashi, and T. Sakuma: *J. Mater. Res.*, 1998, vol. 13, pp. 3449-52.
35. H. Gleiter: *Acta Metall.*, 1969, vol. 17, pp. 565-73.
36. H. Gleiter: *Acta Metall.*, 1969, vol. 17, pp. 853-62.
37. H. Gleiter: *Acta Metall.*, 1969, vol. 17, pp. 1421-28.
38. M.S. Masteller and C.L. Bauer: *Acta Metall.*, 1979, vol. 27, pp. 483-88.
39. S. Tsurekawa, T. Ueda, K. Ichikawa, H. Nakashima, Y. Yoshitomi, and H. Yoshinaga: *Mater. Sci. Forum*, 1996, vols. 204–206, pp. 221-26.
40. P.A. Beck: *Adv. Phys. (Phil. Mag. Suppl.)*, 1954, vol. 3, pp. 245-324.
41. J.P. Hirth and G.M. Pound: *Condensation and Evaporation, Nucleation and Growth Kinetics; Progress in Material Science*, B. Chalmers, ed., Pergamon Press, Oxford, United Kingdom, 1963, vol. 11, pp. 77-148.
42. J.M. Kosterlitz and D.J. Thouless: *J. Phys. C*, 1973, vol. 6, pp. 1181-1203
43. J.M. Kosterlitz: *J. Phys. C*, 1974, vol. 7, pp. 1046-60.
44. H. van Beijeren: *Phys. Rev. Lett.*, 1977, vol. 38, pp. 993-96.
45. J.D. Weeks: *Ordering in Strongly Fluctuating Condensed Matter Systems*, T. Riste, ed., Plenum, New York, NY, 1980, pp. 293-317.
46. P.E. Wolf, F. Gallet, S. Balibar, E. Rolley, and P. Nozières: *J. Phys.*, 1985, vol. 46, pp. 1987-2007.
47. J.W. Christian: *The Theory of Transformations in Metals and Alloys, International Series on Materials Science and Technology*, 2nd ed., Pergamon Press, Oxford, United Kingdom, 1975, vol. 15, pp. 15-20.
48. F. Assmus, K. Detert, and G. Ibe: *Z. Metallkd.*, 1957, vol. 48, pp. 344-49.
49. A.F. Padilha, J.C. Dutra, and V. Randle: *Mater. Sci. Technol.*, 1999, vol. 15, pp. 1009-14.
50. S.P. Hau-Riege and C.V. Thompson: *Appl. Phys. Lett.*, 2000, vol. 76, pp. 309-11.
51. R.W. Cahn and P. Haasen: *Physical Metallurgy*, 3rd ed., North-Holland Physics Publishing, The Netherlands, 1983, pp. 1611-13.
52. F.J. Humphreys and M. Hatherly: *Recrystallization and Related Annealing Phenomena*, Pergamon Press, Oxford, United Kingdom, 1995, pp. 173-220.